Inorganic Chemistry

pubs.acs.org/IC Article

Werner-Type Complexes of Uranium(III) and (IV)

Judith Riedhammer, J. Rolando Aguilar-Calderón, Matthias Miehlich, Dominik P. Halter, Dominik Munz, Frank W. Heinemann, Skye Fortier, Karsten Meyer,* and Daniel J. Mindiola*

Cite This: *Inorg. Chem.* 2020, 59, 2443−2449 Read Online

ACCESS | Metrics & More | Article Recommendations | Supporting Information

ABSTRACT: Transmetalation of the β-diketiminate salt [M][^{Me}nacnac^{Ph}] (M$^+$ = Na or K; ^{Me}nacnac^{Ph-} = {PhNC(CH$_3$)}$_2$CH$^-$) with UI$_3$(THF)$_4$ resulted in the formation of the homoleptic, octahedral complex [U(^{Me}nacnac^{Ph})$_3$] (**1**). Green colored **1** was fully characterized by a solid-state X-ray diffraction analysis and a combination of UV/vis/NIR, NMR, and EPR spectroscopic studies as well as solid-state SQUID magnetization studies and density functional theory calculations. Electrochemical studies of **1** revealed this species to possess two anodic waves for the U(III/IV) and U(IV/V) redox couples, with the former being chemically accessible. Using mild oxidants, such as [CoCp$_2$][PF$_6$] or [FeCp$_2$][Al{OC(CF$_3$)$_3$}$_4$], yields the discrete salts [**1**][**A**] (A = PF$_6^-$, Al{OC(CF$_3$)$_3$}$_4^-$), whereas the anion exchange of [**1**][**PF$_6$**] with NaBPh$_4$ yields [**1**][**BPh$_4$**].

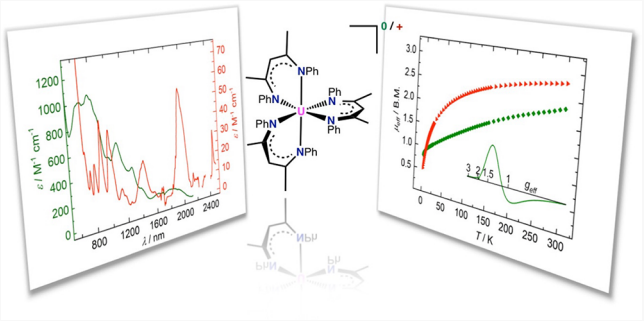

INTRODUCTION

Alfred Werner's disapproval of the complex ion-chain theory proposed by Jørgensen and Blomstrand,[1] via the introduction of coordination complexes and the concept of *Nebenvalenz*,[1,2] resulted in the birth of a field we now term coordination chemistry.[3,4] Soon after, it was realized that the properties of these so-called "complexes" are dictated by their electronic structures. This was understood by an ionic bonding picture called crystal-field theory[5] and, subsequently, by a more sophisticated model that is commonly termed ligand-field theory.[6] More than a century after the introduction of homoleptic and stereoisomeric complexes by Werner (i.e., [Co(*en*)$_3$]Cl$_3$, *en* = H$_2$NCH$_2$CH$_2$NH$_2$ or "hexol" forms),[7,8] we now wish to report the structural, spectroscopic, magnetic, and electrochemical properties of Werner-type chiral complexes of the heaviest naturally abundant metal: uranium. Herein, we report the first examples of homoleptic U(III) and U(IV) ions supported by the β-diketiminate ligand ^{Me}nacnac^{Ph-} (^{Me}nacnac^{Ph-} = {PhNC(CH$_3$)}$_2$CH$^-$, ^{R1}nacnac^{R2}, where R1 is the β-carbon substituent and R2 is the α-N group) and discuss their spectroscopic, magnetic, and electrochemical properties. Solid-state structural studies for these chiral uranium ions are also presented.

Unlike the complexes [U(acac)$_4$][9] and [U(N[R]Ar$_{MeL}$)$_3$], along with the latter's one-electron oxidized counterpart,[10] there are no documented examples of homoleptic Werner-type complexes of uranium with the ubiquitous β-diketiminate ligand.[11] For example, using the more traditional β-diketiminate ligand ^{Me}nacnac^{Dipp-} (^{Me}nacnac^{Dipp-} = {DippNC(CH$_3$)}$_2$CH$^-$, Dipp = 2,6-^{i}Pr$_2$C$_6$H$_3$) results in the formation of monosubstituted complexes, such as [(^{Me}nacnac^{Dipp})UCl$_3$(THF)] and [{(^{Me}nacnac^{Dipp})UCl}$_2$(μ$_2$-Cl)$_3$]Cl.[12] In some cases, disubstitution of ^{Me}nacnac^{Dipp-} generates the rearranged species [(^{Me}nacnac^{Dipp})(η^3-^{Me}nacnac^{Dipp})UI],[13] where one ligand has changed hapticity, most likely due to steric constraints. It has been found that the reactivity of [(^{Me}nacnac^{Dipp})UI$_2$(THF)$_2$] allows for halide substitution, dehydrohalogenation of the β-diketiminate, reduction, and oxidation reactions.[14] Uranyl(VI)- and (V)-based systems have also been reported by this ligand scaffold.[15−18] Whereas the use of the more sterically hindered ligand derivative ^{tBu}nacnac^{Dipp-} (^{tBu}nacnac^{Dipp-} = {DippNC(^{t}Bu)}$_2$CH$^-$) results in only one ligand being incorporated, namely [(^{tBu}nacnac^{Dipp})UCl$_3$].[12] Lappert's {Me$_3$SiNC(Ph)}$_2$CH$^-$ chelate ensues from reactions of ligand cannibalization, forming complexes with 1,3-diaza-allyl ligands.[19] Other examples of uranium complexes using β-diketiminate-like scaffolds include a macrocycle tetramethyltetraazaannulene,[20−22] a dianionic and a tridentate *N*-aryloxy-β-diketiminate,[23] a cyanopentadienyl dianion,[24] and an aza β-diketiminate ligand 2-(4-tolyl)-1,3-bis(quinolyl)-malondiiminate).[25]

On the basis of this precedence, we thought that the use of a less studied and less sterically encumbered β-diketiminate ligand, namely ^{Me}nacnac^{Ph-}, would provide access to homoleptic complexes of uranium.[16] Our goal was to selectively transmetallate three chelating ligands onto the

Received: November 12, 2019
Published: January 24, 2020

https://dx.doi.org/10.1021/acs.inorgchem.9b03229
Inorg. Chem. 2020, 59, 2443−2449

U(III) ion to form D_3 symmetric, enantiomeric pairs. Herein, we present homoleptic examples of U(III) and U(IV) complexes using a phenyl-substituted β-diketiminate ligand and discuss its structural, redox, spectroscopic, and magnetic properties.

RESULTS AND DISCUSSION

Using a modified protocol of one reported in the literature,[26] we developed a convenient entry to the free-base ^{Me}nacnac^{Ph}H in a 47% yield by slowly adding HCl at low temperatures to a mixture of acetylacetone dissolved in aniline.[27] Upon completion of the reaction, the solids must be extracted into CH_2Cl_2 and neutralized with a saturated aqueous solution of Na_2CO_3, and the organic layer separated and then dried with $MgSO_4$; the residue (oily material) is then crystallized from MeOH at −35 °C. The treatment of the crystallized β-diketimine with a slight excess of K{N(SiMe$_3$)$_2$} under an inert atmosphere and in cold Et_2O resulted in the immediate precipitation of a fluffy and voluminous yellow solid, which was isolated, washed with cold Et_2O, dried under vacuum, and subsequently identified to be the salt [K][^{Me}nacnac^{Ph}] on the basis of ^{1}H and ^{13}C NMR spectral data.[27] As represented in Scheme 1, the addition of 3 equiv [K][^{Me}nacnac^{Ph}] (quite

Scheme 1. Synthesis of Homoleptic and Chiral Complexes 1 and [1][X]

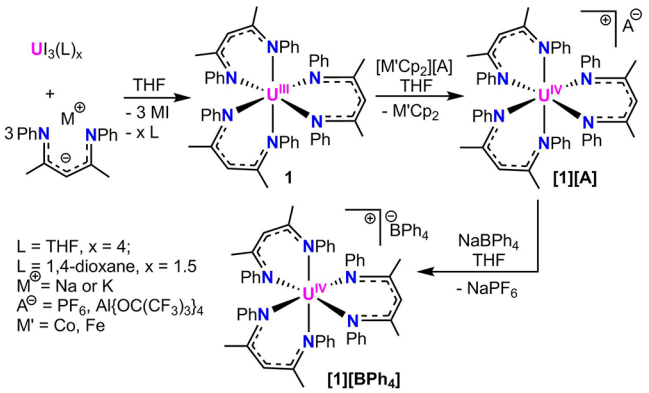

possibly an oligomer containing bridged K-arene units) to either $UI_3(THF)_4$[28] or UI_3(1,4-dioxane)$_{1.5}$[29] and stirring the reaction mixture over 2.5 h at room temperature led to the formation of a dark green solution, from which the complex [U(^{Me}nacnac^{Ph})$_3$] (**1**) was isolated in 71% yield after recrystallization from a concentrated toluene solution at −35 °C.[27] In agreement with its expected D_3 symmetry, the ^{1}H NMR spectrum of **1** reveals this species to possess symmetrically equivalent ligands with three aryl resonances in the aromatic region in addition to one paramagnetically shifted resonance for the β-methyl at −31.63 ppm. The γ-C**H** has not been observed and is likely broadened into the baseline. The X-band EPR spectrum of **1** (Figure 1), recorded in a frozen toluene solution at 9 K, reveals a broad feature (W_1 = 130 mT, W_2 = 120 mT, and W_3 = 140 mT) with rhombic symmetry and simulated effective g values of g_1 = 0.37, g_2 = 1.20, and g_3 = 1.45, in accordance with the complexes' low-temperature magnetic moment (vide infra).

A potentiodynamic electrochemical study (cyclic voltammetry, CV) of **1**, in a THF solution containing [n-NBu$_4$][PF$_6$] as an electrolyte, revealed two redox features at −1.69 and 0.15 V (referenced to $FeCp_2^{0/+}$ at 0.0 V), which was suggestive of

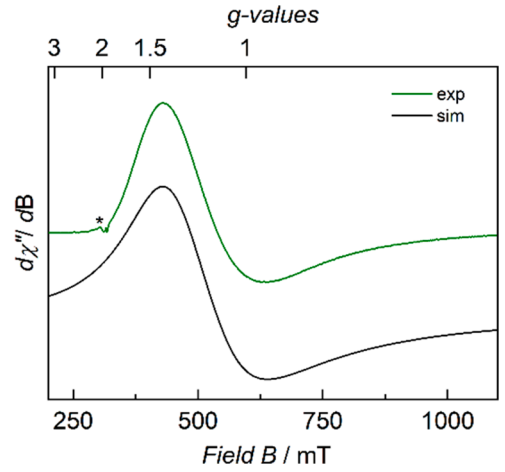

Figure 1. X-band EPR spectrum of **1**, recorded in toluene (40 mM) at 9 K (green trace). Simulation (black trace) gives g_1 = 0.37, g_2 = 1.45, and g_3 = 1.20 with W_1 = 130 mT, W_2 = 120 mT, and W_3 = 140 mT. The background cavity is marked with an asterisk (*).

U(III/IV) and U(IV/V) redox couples, respectively (Figure 2, top). A linear sweep scan also confirmed these two waves to be oxidations (Figure S33). Figure 2 also shows a cathodic wave for **1** above −3 V, but such a feature is clearly irreversible, whereas the first anodic wave, assigned to the U(III/IV)

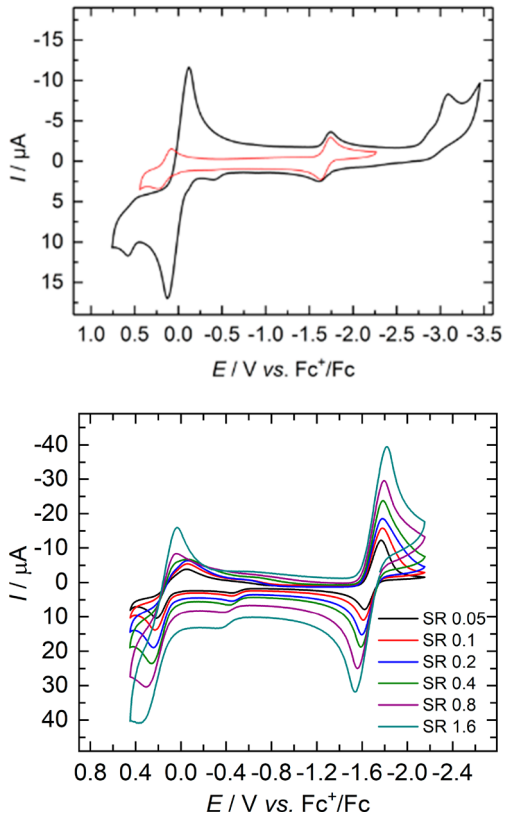

Figure 2. Top: cyclic voltammograms of **1** measured in a THF solution with ∼0.1 M [N(n-Bu)$_4$][PF$_6$] as electrolyte, including the Fc$^+$/Fc redox wave (back trace) and scans of only both oxidations of **1** (red trace). Bottom: cyclic voltammograms of **1** scanned with scan rates (SR) started from 50 mV/s and ended with 1600 mV/s measured in a THF solution with ∼0.1 M [N(n-Bu)$_4$][PF$_6$] as electrolyte.

https://dx.doi.org/10.1021/acs.inorgchem.9b03229
Inorg. Chem. 2020, 59, 2443−2449

couple, is fully reversible at various scan rates from 50 to 1600 mV/s (Figure 2, bottom). The more positive scan at 0.15 V is only quasi-reversible, especially at a higher scan rate of 1600 mV/s (Figure 2, bottom).

Chemical oxidation of **1** with a relatively weak oxidant, such as $[CoCp_2][PF_6]$, resulted in the precipitation of the U(IV) species $[U(^{Me}nacnac^{Ph})_3][PF_6]$ $[\mathbf{1}][\mathbf{PF_6}]$ in an 87% yield with concomitant formation of $CoCp_2$ (Scheme 1). Strangely, for a symmetrical U(IV) ion, the ^{1}H NMR spectrum of $\mathbf{1}^+$, recorded in methylene chloride at 293 K, shows four very broad signals (Figure S6). Similar to **1**, one-electron oxidized $\mathbf{1}^+$ features three aryl resonances in the aromatic region and one paramagnetically shifted resonance for the β-methyl at −1.87 ppm; a resonance for the methine-C**H** could not be detected and assigned.

Complementary to **1**, complex $[\mathbf{1}][\mathbf{PF_6}]$ shows a reversible cathodic and a quasi-reversible anodic wave at −1.82 and 0.23 V (ΔE = 2.05 V), respectively, which were corroborated by a linear sweep scan, showing both anodic and cathodic responses (Figure S39). More soluble variants to $[\mathbf{1}][\mathbf{PF_6}]$, namely $[\mathbf{1}][\mathbf{Al\{OC(CF_3)_3\}_4}]$ (69% yield) and $[\mathbf{1}][\mathbf{BPh_4}]$ (95% yield), could be readily achieved via the oxidation of **1** with $[FeCp_2][Al\{OC(CF_3)_3\}_4]$[27] or alternatively by anion exchange of $[\mathbf{1}][\mathbf{PF_6}]$ with $NaBPh_4$, respectively (Scheme 1). Despite the CV data suggesting the presence of a second and chemically accessible electrochemical oxidation wave for **1**, numerous efforts to chemically access a U(V) salt remained unsuccessful, often resulting in the formation of the free base $^{Me}nacnac^{Ph}H$,[27] which is most likely due to the vulnerability of the $^{Me}nacnac^{Ph-}$ ligand to oxidation and subsequent demetalation.[27] In fact, as shown in Figures S31 and S32, an examination of the scan rate dependence for the second anodic wave of **1** shows the irreversibility in the wave at a scan rate of 50 mV/s, and it is quasi-reversible at much higher scan rates (1600 mV/s). Likewise, the CV data of $[K][^{Me}nacnac^{Ph}]$ reveal an irreversible oxidation wave at −0.4 V, thus arguing for ligand oxidation likely being the locus of reactivity for the second quasi-reversible anodic wave (Figure S34). Given the broad ^{1}H NMR spectral features of both $[\mathbf{1}][\mathbf{PF_6}]$ and $[\mathbf{1}][\mathbf{BPh_4}]$ at room temperature, we conducted variable temperature ^{1}H NMR spectroscopic studies for these two species in the range of 125 to −35 °C (Figures S10−S16).[27] Interestingly, it was found that $\mathbf{1}^+$, regardless of the counter anion, exhibited sharpened signals at higher and at lower temperatures. It is presently unclear why these signals are rather broad at room temperatures.

Solid-state structures of **1**, $[\mathbf{1}][\mathbf{BPh_4}]$, and $[\mathbf{1}][\mathbf{Al\{OC(CF_3)_3\}_4}]$ were collected by single-crystal X-ray diffraction studies with the first two being displayed in Figure 3. Metrical parameters for $[\mathbf{1}][\mathbf{BPh_4}]$ are quite similar to $[\mathbf{1}][\mathbf{Al\{OC(CF_3)_3\}_4}]$ (Table 1), and thus, we omit discussion of the latter complex in the text.[27] Each uranium ion is virtually confined to an octahedral geometry with an overall local D_3 symmetry. As a result of this geometry, the uranium complexes are chiral, with the pair of enantiomers (Λ and Δ) being present in the unit cell, given the centrosymmetric nature of the space group ($P2_1/c$ and $P2_1/n$). Figure 1 (top) shows only the Λ isomer of **1** with the other enantiomer excluded for clarity, in which the U(III) ion is slightly more distorted from that observed for $\mathbf{1}^+$ (Figure 1, bottom) when judged by the U−N distances and N−U−N angles (Table 1). As expected, the oxidation of trivalent **1** to tetravalent $\mathbf{1}^+$ results in a slight shortening of the $U-N_{avg}$ distances from 2.458 to 2.404 Å. This feature is not surprising given the smaller size of the U(IV) ion versus the U(III) ion, but this argues for the oxidation being metal-centered, involving a nonbonding f-orbital. Indeed, density functional theory (DFT) calculations indicate an f^2 electron configuration for the cation $\mathbf{1}^+$ (vide infra and Figure S44).

To further support the uranium ions' formal oxidation states, **1** and $[\mathbf{1}][\mathbf{PF_6}]$ were subjected to spectroscopic and magnetic studies. The UV/vis/NIR electronic absorption spectra of **1**

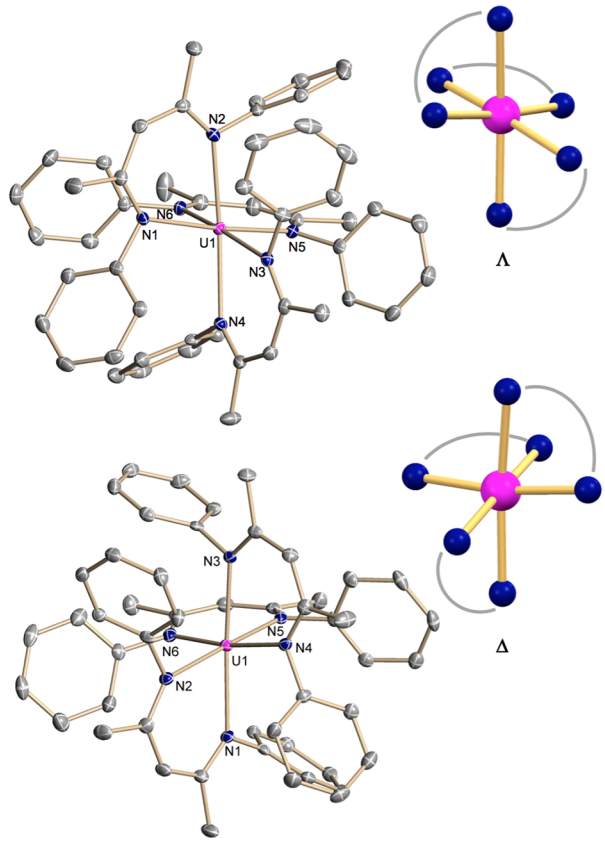

Figure 3. Molecular representation of complexes Λ-**1** (ORTEP, top) and cationic Δ-$[\mathbf{1}][\mathbf{BPh_4}]$ (ORTEP, bottom) in crystals of solvate-free **1** and $[\mathbf{1}][\mathbf{BPh_4}]$ with their first coordination spheres (inserts). All hydrogen atoms and the BPh_4 anion are omitted for clarity. All thermal ellipsoids are shown at the 50% probability level. Only one of the two enantiomers in the unit cell is shown for each complex for the purpose of clarity.

Table 1. Selected Interatomic Distances (Å) and Angles (deg) in 1 and $[\mathbf{1}][\mathbf{BPh_4}]$

	[1]	$[\mathbf{1}][\mathbf{BPh_4}]$
$U-N_{avg}$	2.458	2.404
U−N1	2.458(2)	2.405(2)
U−N2	2.458(2)	2.390(2)
U−N3	2.469(2)	2.405(2)
U−N4	2.450(2)	2.413(2)
U−N5	2.458(2)	2.393(2)
U−N6	2.457(2)	2.420(2)
$\angle_{bite}$ N1−U−N2	73.75(6)	76.03(7)
$\angle_{bite}$ N3−U−N4	74.98(6)	75.02(7)
$\angle_{bite}$ N5−U−N6	74.79(7)	74.79(6)
∠N1−U1−N5 and ∠N2−U1−N5	174.07(6)	172.98(7)
∠N2−U1−N4 and ∠N1−U1−N3	171.90(6)	172.08(7)
∠N3−U1−N6 and ∠N4−U1−N5	170.81(6)	172.88(7)

https://dx.doi.org/10.1021/acs.inorgchem.9b03229
Inorg. Chem. 2020, 59, 2443−2449

and [**1**][**PF**$_6$] were recorded in a spectral range from 250 to 2500 nm. The UV/vis region of **1** and [**1**][**PF**$_6$] (Figure 4) are

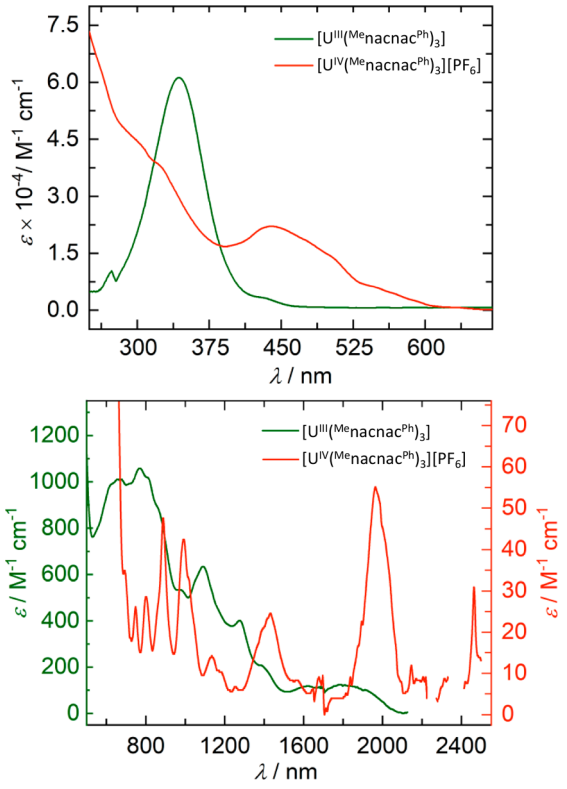

Figure 4. UV/vis/NIR electronic absorption spectra for **1** in toluene (green trace) and [**1**][**PF**$_6$] in methylene chloride (red trace) at 25 °C. Breaks in the NIR spectra are due to cutouts of the solvent absorptions.

dominated by intense absorption bands, and due to their unusually large molar extinction coefficients (ε), these bands are assigned to metal−ligand charge-transfer transitions (either metal-to-ligand or vice versa). Notably, trivalent **1** possesses a well-resolved absorption band centered at 344 nm (ε = 61200 M^{-1} cm^{-1}) with a shoulder at 429 nm (Figure 4, top, green trace). The spectral region between 600 and 2100 nm (Figure 4, bottom) shows a broad band of relatively high intensity centered at 770 nm (ε_{max} = 1060 M^{-1} cm^{-1}), which is often seen for trivalent uranium complexes, albeit at slightly higher energy (500−700 nm),[14,27−30] and this band could be assigned to Laporte-allowed f → d transitions.[30] A number of less-intense, less-resolved Laporte-forbidden f → f transitions are observed on the band's bathochromic flank. The UV/vis spectrum of [**1**][**PF**$_6$] (Figure 4, top, red trace) shows multiple overlapping charge-transfer transitions between 280 and 600 nm, with molar extinction coefficients of ε = 49000 to 18000 M^{-1} cm^{-1}. Characteristic for tetravalent uranium complexes, the NIR region features several sharp f → f transitions with molar extinction coefficients up to ε = 55 M^{-1} cm^{-1} (Figure 4, middle, red trace).[30,31]

The magnetic properties of **1** and [**1**][**PF**$_6$] were determined by SQUID magnetization measurements in the temperature range from 2 to 300 K and with an applied magnetic field of 1 T. For reproducibility, the data were collected on three independently synthesized samples (Figures S19 and S20), and the averaged data plotted as μ_{eff} vs T are shown in Figure 5. The pair of complexes **1**/**1**$^+$ shows characteristic magnetic

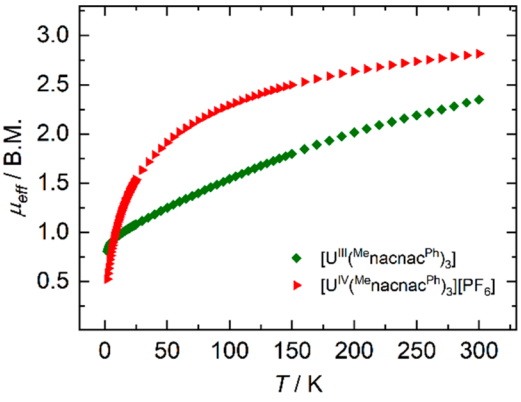

Figure 5. Averaged temperature-dependent magnetic susceptibility data of three independently synthesized samples of **1** (green trace) and [**1**][**PF**$_6$] (red trace), plotted as μ_{eff} vs T (right).

properties for tri- and tetravalent coordination complexes of uranium.[32] The average effective magnetic moment (μ_{eff}) for trivalent **1** is temperature-dependent and varies from 2.35 μ_B at 300 K to 0.80 μ_B at 2 K. The low-temperature value is unusually low for an f^3 complex.[33−36] However, by applying the relation $4\mu_{eff}^2 = (g_1^2 + g_2^2 + g_3^2)$[35] with the experimentally determined effective g values (Figure 1), the resulting value for μ_{eff} is calculated to be 0.96 μ_B, which is in excellent agreement with the experimentally determined magnetic moment of μ_{eff} = 0.95 μ_B at 9 K. Notably, while characteristic for U(IV) f^2 complexes,[32] even in nearly the same ligand environments, the magnetic moment of **1**$^+$ at 300 K is higher than that of its f^3 analogue and was determined to be 2.81 μ_B. Also, typical for U(IV) complexes, the temperature dependence is markedly stronger, which is characteristic of temperature-independent paramagnetism (TIP), with a typical μ_{eff} of 0.52 μ_B at 2 K or even lower; this is in agreement with the complex's nonmagnetic $^3H_4$ ground state.[36]

A computational analysis by DFT was performed in order to further elucidate the electronic structure of **1**.[37] Optimizations of the structural parameters were subsequently performed, where the aryl substituents were truncated by methyl groups (BP86/DKH-def2-SVP). The obtained U−N bond lengths as well as the nacnac N−U−N bond angles were in good agreement with the structural parameters from the solid-state structure; the mean deviation from the solid-state, single-crystal XRD structure was 0.006 Å and 2.2° for the bond lengths and angles, respectively. Molecular orbitals were then obtained from single-point calculations at the B3PW91/DKH-def2-TZVPP//BP86/DKH-def2-SVP level of theory. The calculations suggest an f^3 electron configuration with moderate (Löwdin spin population at uranium of 2.6 electrons) delocalization of the spin density onto the nacnac ligands (Figure 6, top). Very little, if any, discrepancy was observed in the spin densities using various levels of theory, but the BP86-D3/DKH-def2-TZVPP//BP86-D3/DKH-def2-SVP and BP86/DKH-def2-TZVPP//BP86/DKH-def2-SVP levels of theory showed the least difference for truncated and nontruncated models (Table S2). The molecular orbitals obtained from the truncated model system were essentially equivalent to those obtained without truncation. Plotting the three singly occupied molecular orbitals associated with the f-orbitals indicates the mixing of one orbital, namely $f_{y(3x^2-y^2)}$, with some π-orbitals derived from the β-diketiminate ligands. The other two orbitals are essentially metal centered f_{yz}^2 and

https://dx.doi.org/10.1021/acs.inorgchem.9b03229
Inorg. Chem. 2020, 59, 2443−2449

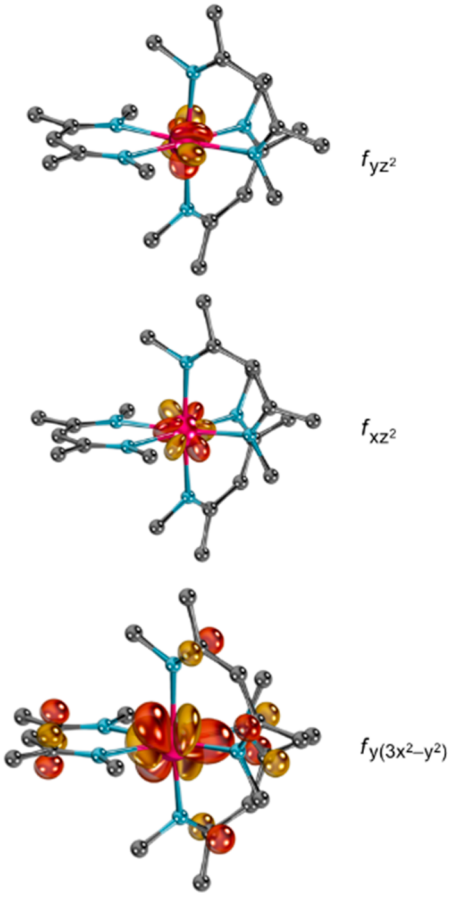

Figure 6. Singly occupied molecular orbitals of **1** (without truncation). Phenyl groups have been omitted for clarity; see Table S2 for calculations without truncation.

f_{xz}^2 orbitals (Figure 6). Conversely, for the U(IV) compound $\mathbf{1}^+$, the B3PW91/DKH-def2-TZVPP//BP86/def2-SVP (U: DKH-def2-TZVP) level of theory was used, and the phenyl groups were not truncated; the mean deviation from the solid-state, single-crystal XRD structure was 0.02 Å and 0.4° for the bond lengths and angles, respectively. It was found that the f^2 electron configuration found in $\mathbf{1}^+$, with f_{yz}^2 and f_{xz}^2 magnetic orbitals (both with some f_z^3 character), has considerable ligand contributions (Figure 7). The greater degree of ligand mixing in the SOMOs of $\mathbf{1}^+$ might help explain why attempts to oxidize this complex result in demetalation.

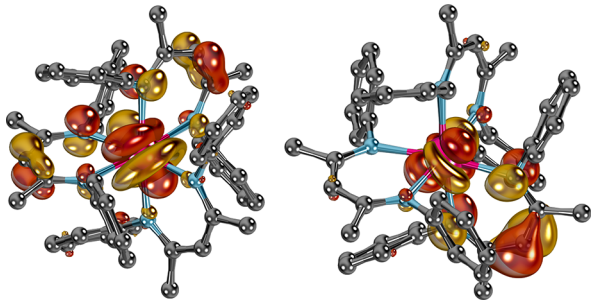

Figure 7. SOMO orbitals for the computed structure of the cation $[\mathbf{1}]^+$ (nontruncated).

CONCLUSION

In summary, we reported the first examples of tris-homoleptic β-diketiminate complexes of uranium. The reduction of steric-bulk by using phenyl groups allows three chelating ligands to coordinate to uranium in a propeller-like fashion, thus rendering these compounds chiral. We also demonstrate how precursor **1** can be smoothly oxidized to $\mathbf{1}^+$ with minimal geometrical rearrangement, when judged by single-crystal solid-state structural studies. Consistent with electrochemical data of complex **1** or $\mathbf{1}^+$, we have been unable to chemically access a hypothetical U(V) complex $[U(^{Me}nacnac^{Ph})_3]^{2+}$. We have shown how complexes **1** and $\mathbf{1}^+$ exist as a pair of enantiomers Λ and Δ, which are observed in the unit cell and are comparable with the findings reported in the literature, namely the complex $[U\{MeC(NCy)_2\}_3]$ by Ephritikhine et al.[38] Spectroscopic and magnetic data for **1** and $\mathbf{1}^+$ are unarguably consistent with f^3 and f^2 ions, which are confined to an idealized D_3 symmetry. Frequency-dependent measurements of the out-of-phase susceptibility $\chi''M$ of **1**, collected with various applied magnetic fields (0.1, 1, and 2 kOe) at AC frequencies of ν = 1−950 Hz from 2−10 K, reveal no single molecular magnetic behavior (Figures S21 and S22). The U(III/IV) complex pair $\mathbf{1}^{0/+}$ presented here compliments the U(V/VI) homoleptic hexakisamide complexes $[U(dbabh)_6]^{0/-}$ (dbabh$^-$ = 2,3:5,6-dibenzo-7-azabicyclo[2.2.1]hepta-2,5-diene), which have been shown to have a reversible U(V/VI) redox couple at −1.01 V.[39]

ASSOCIATED CONTENT

Supporting Information

The Supporting Information is available free of charge on the ACS Publications Web site at DOI: The Supporting Information is available free of charge at https://pubs.acs.org/doi/10.1021/acs.inorgchem.9b03229.

General considerations, synthetic and spectroscopic details, SQUID magnetization data, UV/Vis/NIR electronic absorption spectroscopy, EPR measurements, electrochemical details, references, X-ray crystal structure determinations, references for X-ray structure determination of **1** and $[\mathbf{1}][\mathbf{BPh_4}]$, computational details, and references for computations (PDF)

Accession Codes

CCDC 1943494 for $[U(^{Me}nacnac^{Ph})_3]$ **1**, **CCDC** 1943495 for $[U(^{Me}nacnac^{Ph})_3][BPh_4]$ $[\mathbf{1}][\mathbf{BPh_4}]$, and CCDC 1946325 for $[U(^{Me}nacnac^{Ph})_3][Al\{OC(CF_3)_3\}_4]$ $[\mathbf{1}][\mathbf{Al\{OC(CF_3)_3\}_4}]$ contain the supplementary crystallographic data for this paper. These data can be obtained free of charge via www.ccdc.cam.ac.uk/data_request/cif, by e-mailing data_request@ccdc.cam.ac.uk, or by contacting the Cambridge Crystallographic Data Centre, 12 Union Road, Cambridge CB2 1EZ, U.K. (fax: +44 1223 336033).

AUTHOR INFORMATION

Corresponding Authors

Karsten Meyer − *Inorganic Chemistry, Department of Chemistry and Pharmacy, Friedrich-Alexander-University Erlangen-Nürnberg (FAU), Erlangen 91058, Germany;* orcid.org/0000-0002-7844-2998; Email: karsten.meyer@fau.de

Daniel J. Mindiola − *Inorganic Chemistry, Department of Chemistry and Pharmacy, Friedrich-Alexander-University Erlangen-Nürnberg (FAU), Erlangen 91058, Germany;*

https://dx.doi.org/10.1021/acs.inorgchem.9b03229
Inorg. Chem. 2020, 59, 2443−2449

Department of Chemistry, University of Pennsylvania, Philadelphia, Pennsylvania 19104, United States; orcid.org/0000-0001-8205-7868; Email: mindiola@sas.upenn.edu

Authors

Judith Riedhammer − *Inorganic Chemistry, Department of Chemistry and Pharmacy, Friedrich-Alexander-University Erlangen-Nürnberg (FAU), Erlangen 91058, Germany*

J. Rolando Aguilar-Calderón − *Department of Chemistry and Biochemistry, University of Texas at El Paso, El Paso, Texas 79968, United States; Department of Chemistry, University of Pennsylvania, Philadelphia, Pennsylvania 19104, United States;* orcid.org/0000-0002-3113-3629

Matthias Miehlich − *Inorganic Chemistry, Department of Chemistry and Pharmacy, Friedrich-Alexander-University Erlangen-Nürnberg (FAU), Erlangen 91058, Germany*

Dominik P. Halter − *Inorganic Chemistry, Department of Chemistry and Pharmacy, Friedrich-Alexander-University Erlangen-Nürnberg (FAU), Erlangen 91058, Germany*

Dominik Munz − *Inorganic Chemistry, Department of Chemistry and Pharmacy, Friedrich-Alexander-University Erlangen-Nürnberg (FAU), Erlangen 91058, Germany;* orcid.org/0000-0003-3412-651X

Frank W. Heinemann − *Inorganic Chemistry, Department of Chemistry and Pharmacy, Friedrich-Alexander-University Erlangen-Nürnberg (FAU), Erlangen 91058, Germany;* orcid.org/0000-0002-9007-8404

Skye Fortier − *Department of Chemistry and Biochemistry, University of Texas at El Paso, El Paso, Texas 79968, United States;* orcid.org/0000-0002-0502-5229

Complete contact information is available at: https://pubs.acs.org/10.1021/acs.inorgchem.9b03229

Author Contributions

The manuscript was written through contributions of all authors. All authors have given approval to the final version of the manuscript.

Funding

For funding, we thank the Friedrich-Alexander-University Erlangen-Nürnberg (FAU), the University of Pennsylvania, the US National Science Foundation (CHE-0848248 and CHE-1152123 to D.J.M. and CHE-1827875 to S.F.), and the Welch Foundation (AH-1922-20170325 to S.F). D.J.M. also acknowledges support from the Alexander von Humboldt Foundation. D.M. thanks the "Fonds der chemischen Industrie im Verband der chemischen Industrie" for a Liebig fellowship and the RRZE for computation time.

Notes

The authors declare no competing financial interest.

■ ACKNOWLEDGMENTS

We thank Drs. John C. Huffman and Falguni Basuli for insightful discussions.

■ REFERENCES

(1) Werner, A. Beitrag zur Konstitution anorganischer Verbindungen. *Z. Anorg. Allg. Chem.* **1893**, *3*, 267−330.

(2) Hantzsch, A.; Werner, A. Stereochemical arrangement of atoms in molecules containing nitrogen. *Ber. Dtsch. Chem. Ges.* **1890**, *23*, 11.

(3) The Nobel Prize in Chemistry 1913. https://www.nobelprize.org/prizes/chemistry/1913/summary/ (accessed July 19, 2019).

(4) Constable, E. C.; Housecroft, C. E. Coordination chemistry: the scientific legacy of Alfred Werner. *Chem. Soc. Rev.* **2013**, *42*, 1429−1439.

(5) Bethe, H. Termaufspaltung in Kristallen. *Ann. Phys.* **1929**, *395*, 133−208.

(6) Griffith, J. S.; Orgel, L. E. Ligand-field theory. *Q. Rev., Chem. Soc.* **1957**, *11*, 381−393.

(7) Werner, A. The Asymmetric Cobalt Atom. V. *Ber. Dtsch. Chem. Ges.* **1912**, *45*, 121−130.

(8) Jackson, W. G.; McKeon, J. A.; Zehnder, M.; Neuberger, M.; Fallab, S. The rediscovery of Alfred Werner's second hexol. *Chem. Commun.* **2004**, 2322−2323.

(9) Vallat, A.; Laviron, E.; Dormond, A. A comparative electrochemical study of thorium(IV) and uranium(IV) acetylacetonates. *J. Chem. Soc., Dalton Trans.* **1990**, 921−924.

(10) Fox, A. R.; Silvia, J. S.; Townsend, E. M.; Cummins, C. C. Six-coordinate uranium complexes featuring a bidentate anilide ligand. *C. R. Chim.* **2010**, *13*, 781−789.

(11) A homoleptic tris-phopshinodiboranate complex was recently reported to exist as a mixture of monomer and dimer in solution: Blake, A. V.; Fetrow, T. V.; Theiler, Z. J.; Vlaisavljevich, B.; Daly, S. R. Homoleptic uranium and lanthanide phosphinodiboranates. *Chem. Commun.* **2018**, *54*, 5602−5605.

(12) Monreal, M. J.; Wright, R. J.; Morris, D. E.; Scott, B. L.; Golden, J. T.; Power, P. P.; Kiplinger, J. L. Thorium(IV) and Uranium(IV) Halide Complexes Supported by Bulky β-Diketiminate Ligands. *Organometallics* **2013**, *32*, 1423−1434.

(13) (a) Wright, R. J.; Power, P. P.; Scott, B. L.; Kiplinger, J. L. Uncommon η3-(N,C,C′)-1-Azaallyl Bonding Mode for the Nacnac Ligand: A Bis(β-diketiminato)uranium(III) Iodide Complex. *Organometallics* **2004**, *23*, 4801−4803. (b) Travia, N. E.; Monreal, M. J.; Scott, B. L.; Kiplinger, J. L. Thorium-mediated ring-opening of tetrahydrofuran and the development of a new thorium starting material: preparation and chemistry of $ThI_4(DME)_2$. *Dalton Trans.* **2012**, *41*, 14514−14523.

(14) Wooles, A. J.; Lewis, W.; Blake, A. J.; Liddle, S. T. β-Diketiminate Derivatives of Alkali Metals and Uranium. *Organometallics* **2013**, *32*, 5058−5070.

(15) Wu, G.; Hayton, T. W. Synthesis, Characterization, and Reactivity of a Uranyl β-Diketiminate Complex. *J. Am. Chem. Soc.* **2008**, *130*, 2005−2014.

(16) Wu, G.; Hayton, T. W. Mixed-Ligand Uranyl(V) β-Diketiminate/β-Diketonate Complexes: Synthesis and Characterization. *Inorg. Chem.* **2008**, *47*, 7415−7423.

(17) Schettini, M. F.; Wu, G.; Hayton, T. W. Coordination of N-Donor Ligands to a Uranyl(V) β-Diketiminate Complex. *Inorg. Chem.* **2009**, *48*, 11799−11808.

(18) Schettini, M. F.; Wu, G.; Hayton, T. W. Synthesis and reactivity of a uranyl-imidazolyl complex. *Chem. Commun.* **2012**, *48*, 1484−1486.

(19) Hitchcock, P. B.; Lappert, M. F.; Liu, D.-S. Transformation of the bis(trimethylsilyl)methyl into a 1,3-diaza-allyl ligand. Synthesis and crystal structures of [cyclic] [K{N(R)C(Ar)NC(Ar)CHR}-(NCAr)]$_2$ and [{UCl(μ-Cl)(L)(NR)}$_2$][UCl$_2$(L)(L′)]$_2$ [R = $SiMe_3$; Ar = $C_6H_3Me_2$-2,5; L = [cyclic] N(R)C(Ph)C(H)C(Ph)NR; L′ = [cyclic] N(R)C(Ph)NC(Ph)CHR]. *J. Organomet. Chem.* **1995**, *488*, 241−248.

(20) Hohloch, S.; Garner, M. E.; Parker, B. F.; Arnold, J. New supporting ligands in actinide chemistry: tetramethyltetraazaannulene complexes with thorium and uranium. *Dalton Trans.* **2017**, *46*, 13768−13782.

(21) Hohloch, S.; Garner, M. E.; Booth, C. H.; Lukens, W. W.; Gould, C. A.; Lussier, D. J.; Maron, L.; Arnold, J. Isolation of a TMTAA-Based Radical in Uranium bis-TMTAA Complexes. *Angew. Chem.* **2018**, *130*, 16368−16372.

(22) Pedrick, E. A.; Assefa, M. K.; Wakefield, M. E.; Wu, G.; Hayton, T. W. Uranyl Coordination by the 14-Membered Macrocycle Dibenzotetramethyltetraaza[14]annulene. *Inorg. Chem.* **2017**, *56*, 6638−6644.

(23) Dulong, F.; Thuéry, P.; Ephritikhine, M.; Cantat, T. Synthesis of N-Aryloxy-β-diketiminate Ligands and Coordination to Zirconium, Ytterbium, Thorium, and Uranium. *Organometallics* **2013**, *32*, 1328−1340.
(24) Evans, W. J.; Miller, K. A.; Ziller, J. W. Reductive Coupling of Acetonitrile by Uranium and Thorium Hydride Complexes To Give Cyanopentadienyl Dianion (C6N3H7)2−. *Angew. Chem., Int. Ed.* **2008**, *47*, 589−592.
(25) Chatelain, L.; Mougel, V.; Pecaut, J.; Mazzanti, M. Magnetic communication and reactivity of a stable homometallic cation−cation trimer of pentavalent uranyl. *Chem. Sci.* **2012**, *3*, 1075−1079.
(26) Vicente, I.; Bernardo-Gusmao, K.; Souza, M. O. d.; Souza, R. F. d. Friedel-Crafts alkylation of toluene as a parallel reaction in propylene dimerization catalyzed by nickel β-diimine complex/EASE in homogeneous phase. *J. Braz. Chem. Soc.* **2014**, *25*, 2151−2156.
(27) See the Supporting Information.
(28) Clark, D. L.; Sattelberger, A. P.; Bott, S. G.; Vrtis, R. N. Lewis base adducts of uranium triiodide: a new class of synthetically useful precursors for trivalent uranium chemistry. *Inorg. Chem.* **1989**, *28*, 1771−1773.
(29) Monreal, M. J.; Thomson, R. K.; Cantat, T.; Travia, N. E.; Scott, B. L.; Kiplinger, J. L. UI_4(1,4-dioxane)$_2$, [UCl_4(1,4-dioxane)]$_2$, and UI_3(1,4-dioxane)1.5: Stable and Versatile Starting Materials for Low- and High-Valent Uranium Chemistry. *Organometallics* **2011**, *30*, 2031−2038.
(30) La Pierre, H. S.; Kameo, H.; Halter, D. P.; Heinemann, F. W.; Meyer, K. Coordination and Redox Isomerization in the Reduction of a Uranium(III) Monoarene Complex. *Angew. Chem., Int. Ed.* **2014**, *53*, 7154−7157.
(31) Liddle, S. T. The Renaissance of Non-Aqueous Uranium Chemistry. *Angew. Chem., Int. Ed.* **2015**, *54*, 8604−8641.
(32) Kindra, D. R.; Evans, W. J. Magnetic Susceptibility of Uranium Complexes. *Chem. Rev.* **2014**, *114*, 8865−8882.
(33) Fortier, S.; Walensky, J. R.; Wu, G.; Hayton, T. W. Synthesis of a phosphorano-stabilized U(IV)-carbene via one-electron oxidation of a U(III)-ylide adduct. *J. Am. Chem. Soc.* **2011**, *133*, 6894−6897.
(34) Bart, S. C.; Heinemann, F. W.; Anthon, C.; Hauser, C.; Meyer, K. A New Tripodal Ligand System with Steric and Electronic Modularity for Uranium Coordination Chemistry. *Inorg. Chem.* **2009**, *48*, 9419−9426.
(35) Schmidt, A.-C.; Nizovtsev, A. V.; Scheurer, A.; Heinemann, F. W.; Meyer, K. Uranium-mediated reductive conversion of CO_2 to CO and carbonate in a single-vessel, closed synthetic cycle. *Chem. Commun.* **2012**, *48*, 8634−8636.
(36) Nakai, H.; Hu, X.; Zakharov, L. N.; Rheingold, A. L.; Meyer, K. Synthesis and Characterization of N-Heterocyclic Carbene Complexes of Uranium(III). *Inorg. Chem.* **2004**, *43*, 855−857.
(37) Computations were performed on the B3PW91/DKH-def2-TZVPP//BP86-DKH-def2-SVP level of theory for a model system, where the phenyl groups were truncated by methyl substituents. See the SI for the computational details, an evaluation of the computational method, and the calculations without truncation of the phenyl groups.
(38) Villiers, C.; Thuery, P.; Ephritikhine, M. A comparison of analogous 4f- and 5f-element compounds: syntheses, x-ray crystal structures and catalytic activity of the homoleptic amidinate complexes [M{$MeC(NCy)_2$}$_3$] (M = La, Nd or U). *Eur. J. Inorg. Chem.* **2004**, *23*, 4624−4632.
(39) Meyer, K.; Mindiola, D. J.; Baker, T. A.; Davis, W. M.; Cummins, C. C. Uranium hexakisamido complexes. *Angew. Chem., Int. Ed.* **2000**, *39*, 3063−3066.

https://dx.doi.org/10.1021/acs.inorgchem.9b03229
Inorg. Chem. 2020, 59, 2443−2449